Laboratory investigations of processes in large-scale environmental flows and climate dynamics (FK125024) final report

Miklos Vincze

Introduction

Based on the principle of hydrodynamic similarity many fundamental aspects of Earth's climate system can be modeled using laboratory-scale experimental set-ups. Under laboratory conditions it is possible to control the governing physical parameters and thus to separate different processes that cannot be studied independently in such complex systems as the real atmosphere or oceans. In our research project we have addressed crucially important means of momentum transfer in the oceans and the atmosphere: wind-stress driven mixing, tidally excited internal waves, and coherent material-holding eddies. We have also investigated further climate dynamics-motivated problems focusing on the transitions between different states of a minimal model of the mid-latitude atmospheric circulation. In our proposal, we have defined three main research topics (hereafter referred to as "RT"s), and an additional fourth one (RT4) has emerged naturally throughout the (extended) grant period. In what follows, we summarize the key findings of each RT in separate chapters.

RT1: Experimental demonstration of Ekman layer resonances

The temporal variability of wind stress acting on the ocean surface may have a significant impact on the energy transfer between the surface ocean and the deep ocean. In particular, the surface ocean layer is expected to deepen when the wind's frequency matches the inertial (Coriolis) frequency, through the so-called "Ekman layer resonance". In collaboration with Yosef Ashkenazy (Ben Gurion University, Israel) we created a laboratory analog model setting in the large circular rotating tank of the Coriolis Platform – which, with its 13-meter diameter is Europe's largest rotating fluid dynamic experimental facility, located in Grenoble, France – to investigate the effect of oscillating horizontal shear imposed at the water body by a co-rotating and horizontally oscillating, slightly submerged acrylic plate. The analysis of the flow structure by means of particle image velocimetry (PIV) revealed a resonant thickening of the top Ekman boundary layer and a marked increase in the time "average baroclinic kinetic energy" $\langle KE' \rangle$ of the flow, when the forcing frequency approaches the Coriolis frequency of the rotating tank (Fig.1). The findings are in agreement with our theoretical expectations and constitute evidence for the existence of the Ekman layer resonance (or near inertial resonance) phenomenon in an ocean-like configuration.

For a better understanding of the observed phenomena a new theoretical formulation has also been developed in collaboration with Marten Klein, researcher of the Brandenburg University of Technology (Cottbus, Germany). These novel theoretical results of Ekman resonance in the laminar (or weakly linear) regime were also presented in our publication besides the experimental results.

As an originally unplanned practical offshoot of this research topic focusing on wind-surface interactions and Ekman layer dynamics, we have also analysed wind speed and solar irradiation data of high spatial and temporal resolution for an extended area of north-western Africa including the

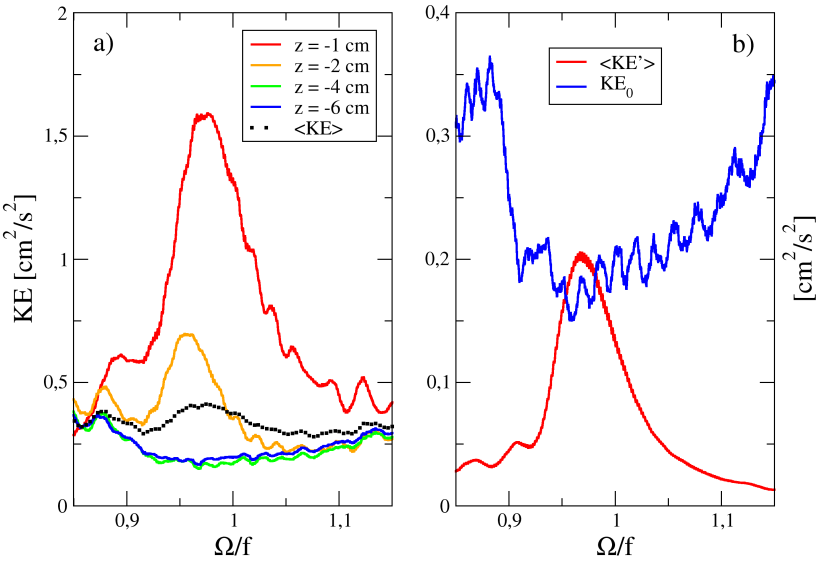

Figure 1: Ekman layer resonance in our Coriolis Platform experiment, as a function of forcing frequency Ω relative to the Coriolis frequency f. Panel (a) shows the time average "kinetic energy" at various depths of the water (see legend). Panel (b) shows the total integrated kinetic energy in the investigated vertical domain, as decomposed to height-independent (barotropic) component KE_0 (blue) and the integrated total height-dependent (baroclinic) part $\langle KE' \rangle$ (red). Source: [1].

Mediterranean Sea using the data bank compiled and maintained by the European Centre for Medium Range Weather Forecast (ECMWF). We demonstrated that the desert area is an optimal location for wind- and solar electricity production for two peculiar aspects. First, the wind speeds at 100 m over the Sahara are almost as large as wind speeds over the open sea. Secondly, there are utilizable anti-correlations between local wind speeds at 100 m height and surface solar radiations over the Sahara. We provided a theoretically optimum combination of the two resources in a simple model framework. We found that resource combinations between 60-40% and 70-30% wind-solar electricity aggregation in a hybrid system would provide an optimally smooth output with a minimal loss of total production achieved by either pure wind or pure photo-voltaic generation.

Our findings related to RT1 have been published in references [1] and [2].

RT2: Nonlinear internal waves in shallow layers

Internal gravity waves play an essential role in the dynamics of natural water bodies ranging from stratified lakes to oceans. Energy and momentum transfer between surface waves and their internal counterparts in the bulk are ubiquitous in nature: exchange flows between differently stratified connected basins, tidal conversion at seafloor sills in the deep ocean, or the so-called dead-water effect that converts the kinetic energy of a moving ship to interfacial wave energy in stratified fjords are just a few examples of its occurrence on different scales.

Coastal areas with river (or glacier) runoff or regions in the open ocean with steep thermocline can be treated as a system of uniform or linearly stratified water layers located stably above each other. Waves propagating along the interfaces between the layers can be either barotropic or baroclinic in nature. In the former case, the vertical oscillations of the considered interface are in phase with that of the water surface and their amplitudes and wave speeds are of the same order of magnitude. In baroclinic waves, however, the internal waves may exhibit large amplitudes without practically any noticeable displacement at the surface. The energy of barotropic flow can be converted to excite baroclinic wave modes in the bulk by the interaction of flow and topography. This process is ubiquitous in the deep ocean and can also exist in enclosed or semi-enclosed basins, e.g., fjords. Stratified fjords

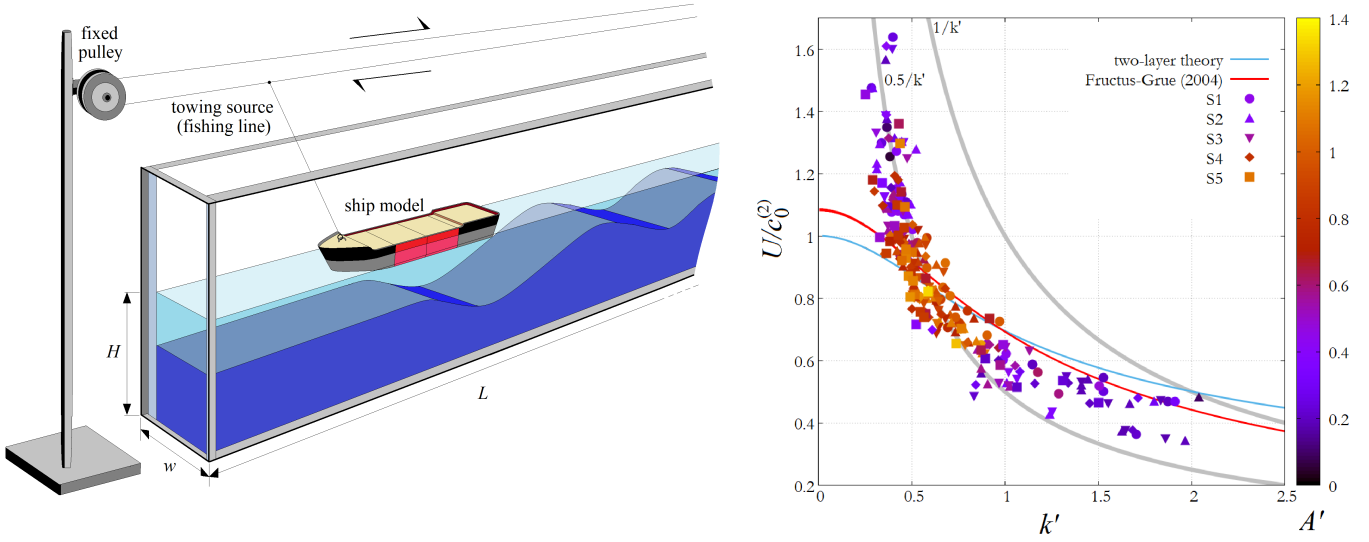

Figure 2: Left: the sketch of the towed ship experiment and the excitation of internal waves along the interface of the two fluid layers underneath the ship model. Right: non-dimensional wavenumber-towing speed diagram with the measured average (non-dimensional) internal wave amplitudes – as coloring – and theoretical dispersion relation relations of different wave types (curves). We found that the amplitudes tend to grow large where the dispersion curves intersect, thus different types of internal waves can be in "constructive interference". Source: [4].

are particularly interesting, because their topography often includes a sill that traps dense seawater in the basin.

We have studied interfacial internal waves in a stratified fluid experiment, driven by periodic free-surface oscillations in a long wavetank. The free-surface waves induced barotropic–baroclinic energy conversion via of a Gaussian sill-like obstacle placed at the bottom of the water tank, imitating seafloor topography. The connection between horizontal surface velocities and internal wave amplitudes was investigated, and the developing flow patterns and the wave speeds of internal waves were systematically analyzed and compared to two- and three-layer theories. We found that despite the fact that the observed internal waves can have considerably large amplitudes, a small amplitude three-layer approximation still gives fairly good agreement with the experimental results.

In the aforementioned "dead water" phenomenon, similar interfacial internal waves are excited in the wake of towed ships, whose dynamics we studied experimentally in a rectangular laboratory tank of quasi-two layer salinity stratified water using a towed model ship (Fig.2a). In the dead water problem, at a critical 'resonant' towing velocity, whose value depends on the structure of the vertical density profile, the amplitude of the internal wave train following the ship reaches a maximum, in unison with the development of a drag force acting on the vessel. The amplitudes and wavelengths of the emerging internal waves were evaluated for various model ship speeds, ship lengths and stratification profiles. We then comapred our results to predictions of linear two- and three-layer theories of freely propagating waves and lee waves. We found that despite the fact that the observed internal waves can have considerable amplitudes, linear theories can still provide a surprisingly adequate description of subcritical-to-supercritical transition and the associated amplification of internal waves. We argued that the latter can be interpreted as a coalescence of frequencies of two fundamental stable wave motions, namely lee waves and propagating interfacial wave modes (Fig.2b).

In a third series of experiments, we addressed the "seiche damping" problem, in which standing waves (seiches) are excited at the free surface of a stratified water body. We analyzed the damping rate of these surfaces waves and evaluated the results as a function of the parameters of the applied salinity stratification profile and the properties of different bottom obstacles in our experimental tank. We found that, in agreement with the expectations, the presence of a "seabed" sill whose height roughly

coincides with the internal pycnocline of the 2-layer system indeed yields significantly faster decay than the ones observed in obstacle-free control run, due to the aforementioned barotropic-baroclinic energy conversion. However, the decay rates were found to be especially high if a certain resonance-like "source-filter interaction" can occur between the surface waves and their internal counterparts. If the frequency of the forcing surface mode was such that it can excite internal seiche modes in the bulk, then the decay got radically faster. In other words, that topography-induced baroclinic wave drag contributes markedly to seiche damping in such systems.

Two major pathways of barotropic– baroclinic energy conversions were observed: the stronger one — involving short-wavelength internal modes of large amplitudes — may occur when the node of the surface seiche is situated above the close vicinity of the sill. The weaker, less significant other pathway is the excitation of long waves or internal seiches along the pycnocline that may resonate with the low-frequency components of the decaying surface forcing.

We analyzed the implications and applicability of these findings to actual sill fjords in nature, e.g., the Gullmar fjord of Sweden, whose internal wave excitation dynamics served as the motivation for our work. We concluded that our findings are of relevance for the better understanding of internal wave excitation in quasi-two-layer sill fjords, as they demonstrate that the waves generated in such systems can be treated fairly well using the dispersion relations of the linear two-layer theory in cases where the surface forcing frequencies are large, e.g., in earthquake-induced fjord seiches. We also demonstrated that in this particular system, nonlinear corrections to internal wave speeds are negligible, despite the fact that internal wave amplitudes are often comparable to the characteristic vertical scale of the stratification, similarly to the case of natural sill fjords.

Our findings related to RT2 have been published in references [3, 4, 5].

RT3: Conceptual models of flow regime transitions in the mid-latitude planetary circulation

The differentially heated rotating annulus is a widely studied experimental model of the mid-latitude atmospheric and ocean circulation in which the fundamental underlying dynamics of baroclinic instability, Rossby waves, and cyclogenesis, circumpolar jets, etc. can be reproduced to a conceptual level, obeying the principle of hydrodynamic similarity.

The cylindrical tank is mounted on a turntable revolving around its axis of symmetry, and is divided into three sections by heat conductive coaxial cylindrical walls. The innermost domain is referred to as the "cold bath", where water of constant temperature is circulated through a cooling thermostat (chiller). A separate regulated closed loop water circuit keeps the "warm bath", i. e. the outermost annular gap, and its sidewall at a higher prescribed temperature. The inner annular cavity forms the experimental domain, and is filled up with water. The fluid surface is free, and the flow is driven by the buoyancy flux maintained by the temperature contrast between the cylindrical walls. This configuration is a barebone representation of the atmosphere at the mid-latitudes of the Northern Hemisphere with the inner "cold" cylinder modeling the cold polar regions and the "warm" outer rim the subtropics (Fig.3a).

We have carried out systematic search for inertial gravity waves (IGWs) connected to the cyclonic and aticyclonic eddies of thermal Rossby waves in this experimental configuration both in laboratory experiments and numerical simulations with our collaborators in BTU Cottbus, FU Berlin and the CNRS IRPHE institute in Marseille. Small-scale wave trains were observed, attached to the meandering jet around the Rossby wave, indicating the presence of an imbalance of the large-scale quasi-geostrophic flow and IGW excitation. These experiments were the firsts of their kind where the simultaneous occurrence of different wave types (Kelvin-, Poincaré-waves and IGWs) was observed and reported in detail in a laboratory setting.

We have also investigated a modified version of the classic annulus experiment, in which a jux-

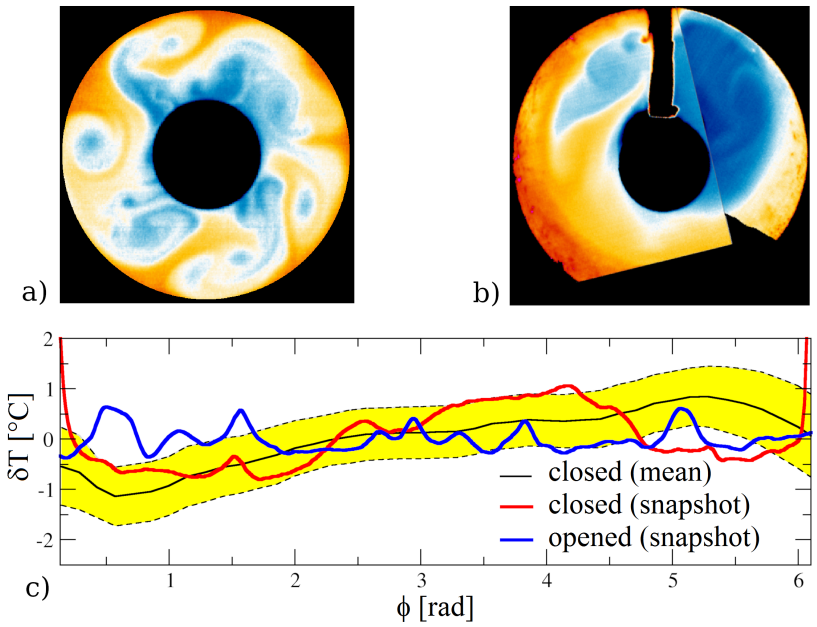

Figure 3: Exemplary infrared camera images of the surface temperature anomaly fields of the differentially heated rotating annulus the "open" (a) and "closed" (b) configurations. The inner cylinder (black circle in the center) is cooled whereas the outer rim of the cylindrical tank is heated, thus providing buoyancy forcing for the circulation. (c) Mid-radius azimuthal temperature anomaly profiles ex- tracted from the data of panels a) and b) (blue and red, respectively) and the time-averaged azimuthal profile of the 'closed' configuration as measured with an infrared sensor. Source: [8].

taposition of convective and motionless stratified layers was created by introducing a vertical salt stratification. The thermal convective motions were suppressed in a central region at mid-depth of the rotating tank, therefore double-diffusive convection rolls could develop in thin layers located at top and bottom, where the salt stratification was the weakest. For high enough rotation rates, the baroclinic instability destabilised the flow in the top and the bottom shallow convective layers, generating cyclonic and anticyclonic eddies separated by the stable stratified layer.

This allows the study of momentum and energy exchange between the layers, primarily by the propagation of IGWs. We used PIV velocity maps (using a co-rotating laser and camera) to describe the wavy flow pattern at different heights. The signature of small-scale IGWs could also be observed attached to the meandering baroclinic jet. The baroclinic waves occured at the thin convectively active layer at the surface and the bottom of the tank, though decoupled they showed different manifestation of nonlinear interactions.

Our findings contribute to a better understanding of the life cycle of IGWs generated in the atmosphere and in the deep ocean. Thanks to the alternation of conductive and stably stratified layers, this experiment configuration resembles the convective and radiative layers of stars, the atmospheric troposphere and stratosphere, or turbulent layers at the sea surface above stratified waters.

We also have conducted two further paleoclimate-inspired experimental campaigns using another modified version of the classical rotating annulus set-up, where we inserted an insulating "meridional" to block zonal circulation. This experiment served as a minimal model of the Southern Ocean with a closed Drake Passage, imitating the situation before the Eocene-Oligocene Transition (EOT) ca. 34 million years ago. The obtained temperature fields and time series were compared to the ones from control runs with partially blocked and fully opened "passages" (Fig.3b). In the closed case a persistent azimuthal temperature gradient was found to emerge (Fig.3c), whose magnitude scales linearly with the 'meridional' temperature contrast. The anomalous temperature distribution was accompanied with perturbations of the background flow yielding significantly larger low frequency variability than in the opened configuration. These findings have implications to the EOT, e.g.

they indicate that there may had been a significant temperature contrast between the water of the Atlantic and Pacific Oceans before the Drake Passage has fully opened. At present the validation of these consequences is hindered by the lack of deep-sea drilling data from the Southeast Pacific and adjacent parts of the Southern Ocean. Our model may inspire further paleoceanographic research in this largely unexplored region.

Our second measurement campaign targeting the dynamics of EOT has investigated the relationships between water surface temperature and the Drake Passage opening. Besides experimental modeling, the problem was also being tackled using the Planet Simulator (PlaSim) intermediate complexity Global Climate Model (GCM).

Although EOT is associated with a pronounced global cooling, our experimental results have shown that – seemingly contradicting paleoclimate records – opening the pathway in the laboratory model yields higher values of mean water surface temperature than the "closed" configuration. This mismatch pointed to the importance of the role ice albedo feedback plays in an EOT-like transition, a component that could not be captured in the laboratory model. Our conclusion was supported by numerical runs performed in the aforementioned PlaSim model, where both "closed" and ¨open" configurations were simulated, with and without active sea-ice dynamics. The numerical results indicated that sea surface temperatures would change in the opposite direction following an opening event in the two ice-dynamics settings, and the results are therefore consistent both with the laboratory experiment (slight warming after opening) and the paleoclimatic data (pronounced cooling after opening). This finding provides circumstantial evidence supporting a particular EOT scenario in which Antarctica has already been — at least partially — covered with ice when the Drake Passage fully opened.

We also used rotating annulus set-ups to investigate the effect of polar warming on the mid-latitude jet stream experimentally. Our results have shown that a progressive decrease in the meridional temperature difference has slowed down the eastward propagation of the jet stream and complexifies its structure. At the same time, temperature variability has decreased in relation to the laboratory-scale "Arctic warming" only at locations representing the Earth's polar and mid-latitudes, which were influenced by the jet stream, whilst the trend reversed in the subtropical region south of the simulated jet. Reduced variability results in narrower temperature distributions and hence milder extreme events. However, our experiments also have shown that the frequency of such events increases at polar and mid-latitudes with decreased meridional temperature difference, whereas it decreases towards the subtropics. Despite missing land–sea contrast in the laboratory model, we have found qualitatively similar trends of temperature variability and extreme events in the experimental data and the National Centers for Environmental Prediction (NCEP) reanalysis data.

Our findings related to RT3 have been published in references [6, 7, 8, 9, 10, 11].

1 RT4: Vortex dynamics in experiments and ocean field data

As an offshoot of RT3 – inspired by the observation that the cyclonic and anticyclonic eddies in the baroclinic annulus appeared to be very persistent coherent structures — we started to investigate the general material-holding properties of geophysical vortices in a simpler experimental setting – by injecting dye into a vertical vortex generated by a commercial magnetic stirrer in a cylindrical tank of water. We found that dye remained captured around the vortex core over minutes, while it got mixed with the water outside this region rather rapidly. Thus, considering its horizontal motion, the dye has become trapped within a critical radius, even though the vortex structure (and the dyed region) was aperiodically time-dependent due to the oscillations of the position of the stirring bar (Fig.4).

According to recent theoretical works by the group of G. Haller (ETH, Zürich) three-dimensional time-dependent vortices should be defined as rotating, material-holding tubular regions of the fluid. To

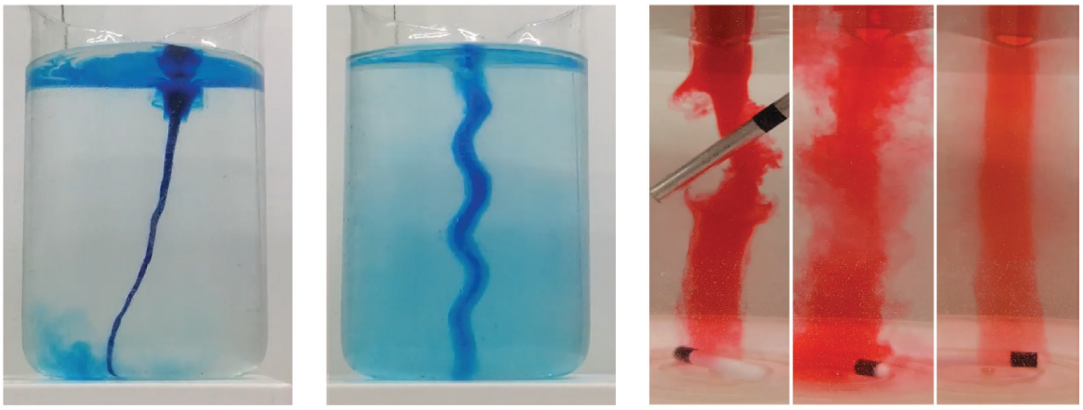

Figure 4: A demonstration of the extreme stability of a three dimensional vortex as a "Lagrangian Coherent Structure". A vortex captures dye even if it is tilted (a), if it becomes a snake vortex after 'kicking' the container, or if it is cut through by a rod (c). Source: [13].

the best of our knowledge, our vortex experiments have provided the first pieces of evidence supporting this theory in a dedicated laboratory experiment. Our data have also provided information about quantities not predicted by the theory, e.g., the lifetime of dye spent within the vortex. We have shown that the maximum radius of the stable dye cylinders, i.e., the horizontal extent of the vortex, hardly depends on the rotational frequency of the stirrer bar — at least in the range investigated — but increases with the length of the bar. A generalization of this finding led to the conclusion that the size of the material-holding region of the vortices in nature should be proportional to the size of the surface (or pressure) depression accompanying the vortex.

We have also analyzed the persistent mesoscale eddies in the open ocean with diameters of around 100 km using satellite-based ocean surface elevation data. These eddies transport a huge amount of heat and material and are therefore key elements of the "weather" of the ocean. From field data from large regions of the Pacific, we calculated the total energy of the near-surface flows and the percentage "stored" in the swirling motion. This percentage has been found to be universal for various off-shore regions. This universality implies that the combined global effect of all mesoscale eddies can be treated as a single strong "super-vortex". This finding is rather helpful to estimate the energy budget of ocean regions where only sparse field data is available.

Our findings related to RT4 have been published in references [12, 13, 14, 15].

References

[1] Vincze, M., N. Fenyvesi, M. Klein, J. Sommeria, S. Viboud, and Y. Ashkenazy. 2019. "Evidence for Wind-Induced Ekman Layer Resonance Based on Rotating Tank Experiments." EUROPHYSICS LETTERS 125 (4). doi:10.1209/0295-5075/125/44001.

[2] Jánosi, Imre M., Karim Medjdoub, and Miklós Vincze. 2021. "Combined Wind-Solar Electricity Production Potential over North-Western Africa." RENEWABLE SUSTAINABLE ENERGY REVIEWS 151. doi:10.1016/j.rser.2021.111558.

[3] Vincze, M, and T Bozóki. 2017. "Experiments on Barotropic–baroclinic Conversion and the Applicability of Linear N-Layer Internal Wave Theories." EXPERIMENTS IN FLUIDS 58 (10). doi:10.1007/s00348-017-2418-7.

[4] Medjdoub, Karim, Imre M. Jánosi, and Miklós Vincze. 2019. “Laboratory Investigations on the Resonant Feature of ‘dead Water’ Phenomenon.” EXPERIMENTS IN FLUIDS 61 (1). doi:10.1007/s00348-019-2830-2.

[5] Medjdoub, Karim, Imre M. Jánosi, and Miklós Vincze. 2021. “Laboratory Experiments on the Influence of Stratification and a Bottom Sill on Seiche Damping.” OCEAN SCIENCE 17 (4): 997–1009. doi:10.5194/os-17-997-2021.

[6] von Larcher, Thomas, Stephane Viazzo, Uwe Harlander, Miklos Vincze, and Anthony Randriamampianina. 2018. “Instabilities and Small-Scale Waves within the Stewartson Layers of a Thermally Driven Rotating Annulus.” JOURNAL OF FLUID MECHANICS 841: 380–407. doi:10.1017/jfm.2018.10.

[7] Rodda, C., I. D. Borcia, P. Le Gal, M. Vincze, and U. Harlander. 2018. “Baroclinic, Kelvin and Inertia-Gravity Waves in the Barostrat Instability Experiment.” GEOPHYSICAL AND ASTROPHYSICAL FLUID DYNAMICS 112 (3): 175–206. doi:10.1080/03091929.2018.1461858.

[8] Bozóki, Tamás, Levente Czelnai, Attila Horicsányi, Anita Nyerges, András Pál, József Pálfy, and Miklós Vincze. 2019. “Large-Scale Ocean Circulation in the Southern Hemisphere with Closed and Open Drake Passage – A Laboratory Minimal Model Approach.” DEEP-SEA RESEARCH PART II-TOPICAL STUDIES IN OCEANOGRAPHY 160 (SI): 16–24. doi:10.1016/j.dsr2.2019.01.005.

[9] Vincze, Miklós, Bozóki T., Mátyás Herein, Borcia I. D., Harlander U., Horicsányi A., Anita Nyerges, Rodda C., Pál A., and József Pálfy. 2021. “The Drake Passage Opening from an Experimental Fluid Dynamics Point of View.” SCIENTIFIC REPORTS 11 (1). doi:10.1038/s41598-021-99123-0.

[10] Rodda, Costanza, Uwe Harlander, Miklos Vincze, 2022. “Jet stream variability in a polar warming scenario–a laboratory perspective.” Weather and Climate Dynamics, 3, 937–950. doi:10.5194/wcd-3-937-2022

[11] Harlander, Uwe, Ion Dan Borcia, Miklos Vincze, and Costanza Rodda. 2022. “Probability Distribution of Extreme Events in a Baroclinic Wave Laboratory Experiment.” FLUIDS 7 (8). doi:10.3390/fluids7080274.

[12] Tel, T, L Kadi, IM Janosi, and M Vincze. 2018. “Experimental Demonstration of the Water-Holding Property of Three-Dimensional Vortices.” EUROPHYSICS LETTERS 123 (4). doi:10.1209/0295-5075/123/44001.

[13] Tél, T, M Vincze, and I M Jánosi. 2020. “Vortices Capturing Matter: A Classroom Demonstration.” PHYSICS EDUCATION 55 (1). doi:10.1088/1361-6552/ab4d25.

[14] Jánosi, Imre M., Miklós Vincze, Tóth Gábor, and Jason A. C. Gallas. 2019. “Single Super-Vortex as a Proxy for Ocean Surface Flow Fields.” OCEAN SCIENCE 15 (4): 941–949. doi:10.5194/os-2019-14.

[15] Janosi, Imre M., Holger Kantz, Jason A. C. Gallas, and Miklos Vincze. 2022. “Global Coarse-Grained Mesoscale Eddy Statistics Based on Integrated Kinetic Energy and Enstrophy Correlations.” OCEAN SCIENCE 18 (5): 1361–1375. doi:10.5194/os-18-1361-2022.